Results in Physics 7 (2017) 1446–1451

Contents lists available at ScienceDirect

Results in Physics

journal homepage: www.journals.elsevier.com/results-in-physics

Chloride effects on the electrochemical degradation of micro-alloyed steel in E20 simulated fuel ethanol blend

Olufunmilayo O. Joseph

Department of Mechanical Engineering, College of Engineering, Covenant University, P.M.B. 1023, Canaanland, Ota, Nigeria

ARTICLE INFO

Article history:
Received 7 March 2017
Accepted 8 April 2017
Available online 18 April 2017

Keywords:
Fuel ethanol
Corrosion
Micro-alloyed steel
Chloride
Pitting

ABSTRACT

Biofuels play a major role as a renewable energy source in mitigating global warming. The presence of impurities in fuel ethanol has resulted into certain downsides regarding material compatibility. This work is focused on an investigation of the influence of sodium chloride (NaCl) as an impurity in the electrochemical degradation of micro-alloyed steel (MAS) when exposed to E20 simulated fuel grade ethanol (SFGE) environment. Immersion and electrochemical tests were carried out using NaCl concentrations ranging from 0 to 64 mg/L. Highest corrosion rates were obtained with 64 mg/L NaCl and lowest rates were observed in the zero chloride tests. Chloride was also seen to cause pitting corrosion on MAS. The results of potentiodynamic polarization tests on MAS compared well with mass loss corrosion rates. Analysis of variance (ANOVA) test confirms the significance of the results at 99% confidence, and further showed that there is significant difference between the chloride concentrations. However, from the perspective of corrosion in fuel ethanol, micro-alloyed steel is thought to be compatible with E20 since the determined corrosion rates were very low.
© 2017 The Author. Published by Elsevier B.V. This is an open access article under the CC BY-NC-ND license (http://creativecommons.org/licenses/by-nc-nd/4.0/).

Introduction

The existence of aggressive ions such as chloride ions in oil and gas environments imposes severe restrictions on the pipeline steels used for such environments due to the corrosion it causes [1]. Chloride ions induce localized corrosion in the steel structures, resulting in the formation of significant amounts of corrosion products [2]. Several studies have been carried out with the aim of determining the resistance of steels to chloride enhanced corrosion [3–5]. In one of the studies [4], corrosion rate was found to increase with increasing chloride and pitting was initiated at highest concentration of chloride. In another study [5] decreasing corrosion rate was observed in the presence of chloride, due to the passivation effect of the oxide layer formed.

Over the last decade, the use of fuel ethanol as a substitute for petrol has increased in several countries, in a bid to decrease fuel emissions and their influence on the environment. However, the presence of sodium chloride in fuel ethanol has contributed to numerous corrosion and stress corrosion cracking incidents at distribution systems and end-user terminals [6]. Oxygen solubility has been found to escalate in ethanol by a substantial quantity relative to aerated ethanol due to the presence of chloride but decreased with increased chloride [7]. Chloride also promotes SCC initiation and growth [7–9]; nonetheless, it does not seem to have any significant effect on crack growth rates [7,10]. A report from another study [11] shows that increased chloride causes initiation and development of pits by breakdown of passive films. Generally, the effect of impurities present in fuel ethanol, such as chloride, acetic acid, sulphur and peroxide positions some limitations concerning material compatibility with fuel ethanol [12–14].

Following the rule of material selection, proper consideration must be given to every stage of material design, manufacture and operation. Of fundamental requirement is the specification of materials which combine corrosion resistance with high mechanical strength [15]. Micro-alloyed steels have wide applications, particularly in automotive industry, ship plates, gas-transmission pipelines, electrical power transmission poles, bridge beams, amongst others [1]. They are called micro-alloyed steels because they contain only a small number of alloying elements: vanadium, niobium or titanium. In addition, they have a ferritic matrix with extremely fine grained structure due to the effects of the alloying elements [16]. Consequently, micro-alloyed steels are generally characterized by high strength and ductility resulting from the fine grains and ferrite matrix. Micro-alloyed steels are thus widely used in the oil and gas industry due to their beneficial mechanical properties. Nevertheless, there is scarce literature vis-à-vis the

E-mail addresses: funmi.joseph@covenantuniversity.edu.ng, lizajose960@gmail.com

http://dx.doi.org/10.1016/j.rinp.2017.04.010
2211-3797/© 2017 The Author. Published by Elsevier B.V.
This is an open access article under the CC BY-NC-ND license (http://creativecommons.org/licenses/by-nc-nd/4.0/).

electrochemical degradation of micro-alloyed steels in fuel ethanol environments.

In view of the above, this study was undertaken to assess the electrochemical degradation of micro-alloyed steel in E20 simulated fuel ethanol environment. In the investigation, corrosion rates from immersion tests and anodic polarization of MAS in the fuel ethanol environment of interest were evaluated. The effect of chloride was also determined by conducting the ethanol-based tests in the presence and absence of chloride.

Materials and methods

Materials and test environments

Samples for experimental analysis were sectioned from new micro-alloyed steel plates in as-received condition. The steel consisted of the following chemical composition (wt.%): C (0.13), Mn (0.77), Si (0.012), Cr (0.027), Ni (0.015), Al (0.042), Ti (0.0025), Mo (0.0017), Cu (0.006) and the balance Fe. E20 + 0 mg/L NaCl (control), E20 + 32 mg/L NaCl, and E20 + 64 mg/L NaCl blends were used for immersion and electrochemical tests. The simulated fuel ethanol test solution was prepared somewhat in line with ASTM D-4806-07 for fuel grade ethanol [17–19] using analytical reagents according to [18]. Unleaded gasoline was used as denaturant. The reference line composition for the SFGE used in this study is shown in Table 1. Chloride concentration was adjusted to simulate the various test conditions. The corrosion tests were carried out at room temperature of 27 °C, under aerated conditions.

Immersion test

Flat square coupons of dimensions 30 mm × 30 mm × 11 mm were machined from new micro-alloyed steel plates for immersion tests. The surfaces of the specimens were ground up to 800 grit, degreased with acetone, and used instantaneously for testing. Measurements of the samples' area and initial weight were taken before exposure to solution. Duplicate samples for each test condition were immersed in solution for a period of 60 days. A total of six samples were used for the test. Each sample was then suspended in solution with nylon thread in closed plastic containers.

The solution was replenished fortnightly to curtail variations in solution composition and make up for evaporation. At the completion of immersion tests, the samples were removed and dried out in warm air. Oxide layers formed on the samples were mechanically scraped off, and chemical cleaning of the samples with Clark's solution followed. Clark's solution was prepared as reported in literature and in line with ASTM Standard G1-03 [18,20]. Final weight measurements were taken after cleaning and an average value was computed for mass loss from each pair of duplicate test. Calculation of corrosion rate was carried out in mils per year (mpy) with Eq. (1) in line with ASTM G1-03 [20]:

$$\text{Corrosion Rate} = (K \times W)/(A \times T \times D) \quad (1)$$

where $K = 534$, W is mass loss (milligrams), A is area (square inches), T is time of exposure (hours) and D is density (g/cm^3).

Electrochemical measurements

Potentiodynamic polarization measurements were carried out using a Gamry reference 600 Potentiostat/Galvanostat/ZRA as reported in [18]. Saturated calomel electrode (SCE) was used as the reference electrode and platinum wire shielded with a glass frit as a counter electrode. Each experiment was carried out in duplicate in order to determine the reproducibility of the experiments. The samples were mounted with Bakelite with the aim of the reducing exposed area. Surfaces of mounted samples were then polished up to 2000 grit and degreased with acetone. Afterwards, the samples were suspended in the ethanolic solution by means of a threaded carbon steel rod. The steel rod was isolated from the test solution with a Teflon tape. To minimize the effect of high solution resistance concomitant with ethanol environments, the test setup was designed in a manner as to maintain constant minimal distance between the working electrode and the reference electrode for all the tests. To guarantee similar reduced metal surface, all the polarization tests began with cathodic polarization at −0.75 V vs SCE. In order to minimize the outcome of chloride seepage from Vycor glass [11,8], 2 mV/s was used as the scan rate.

Microstructure and X-ray diffraction analysis

The surface morphology of the tested samples were characterized after corrosion using a FEI-430 NOVA NANO FEG-SEM. The oxide layers obtained from the immersion tests samples were analysed via a Bruker D8 Discover X-ray diffractometer (XRD). Scan range was set from 10° to 40°. To determine the properties of the corrosion products, the peak patterns obtained from the diffractogram was compared with a large set of standard data. Analysis of the diffractogram obtained was carried out with a software installed on the computer connected to the XRD equipment as described in [18].

Results and discussion

Effect of chloride concentration on mass loss corrosion rates of MAS

The effect of chloride concentration on mass loss corrosion rates of MAS was determined after 60 days' immersion tests on duplicate samples for each test condition. The concentration of chloride was methodically altered to enable determination of the effect of its variation on corrosion rates of the steels. This was realized by means of 0, 32 and 64 mg/L chloride ion (Cl^-) concentrations. Zero chloride tests represented the control test. Fig. 1 shows the influence of changing chloride concentration on the corrosion rate of MAS in E20 fuel ethanol blend. In fuel ethanol, the presence of chloride ions (Cl^-) is thought to originate possibly from the salt used in the preparation of meals in the course of biofuel production [21]. Chloride ions induce localized corrosion on carbon steels and can as well lead to the formation of significant amount of corrosion products on steels [2].

MAS, when immersed in E20 without NaCl, showed a corrosion rate of 8.17×10^{-3} mils per year (mpy). However, increasing the concentration of chloride in E20 resulted in increased corrosion rate of MAS. At 32 mg/L NaCl, corrosion rate increased from 8.17×10^{-3} mpy to 1.25×10^{-2} mpy and upon addition of 64 mg/

Table 1
Baseline composition of SFGE used for the tests [17,18].

Ethanol (Vol%)	Methanol (Vol%)	Water (Vol%)	NaCl (mg/L)	Acetic acid (mg/L)
98.5	0.5	1	32	56

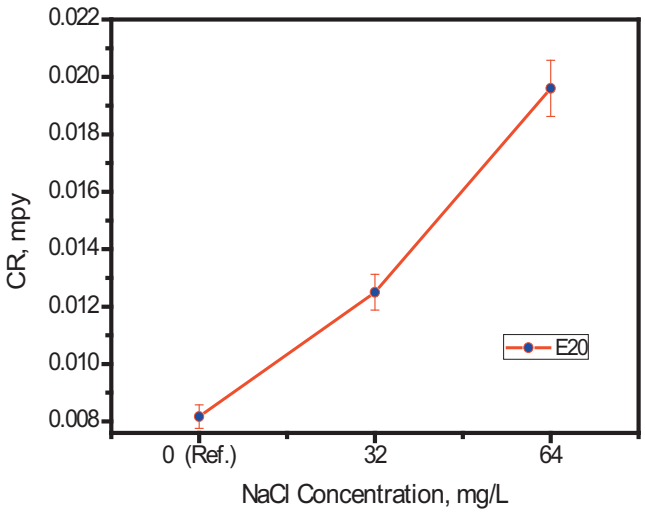

Fig. 1. Effect of chloride concentration on mass loss corrosion rate of MAS in E20 SFGE. Error bars display standard deviation.

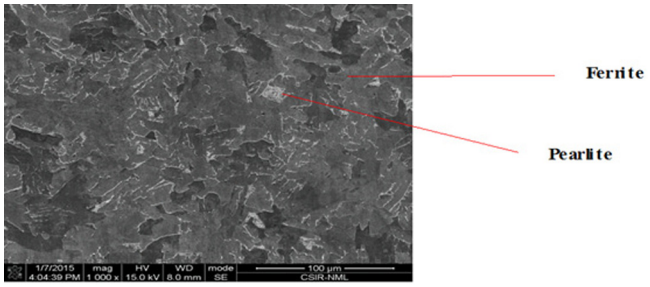

Fig. 2. SEM image of MAS at 1000x in as-received condition.

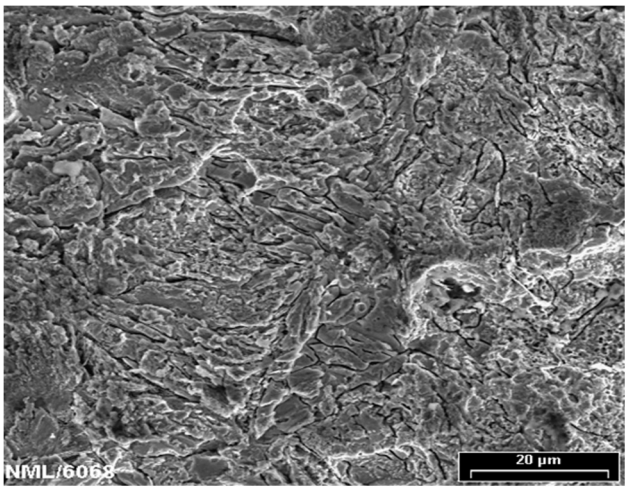

Fig. 3. Shrinkage on surface of MAS after exposure to E20 without chloride.

L NaCl to E20, a higher corrosion rate of 1.96×10^{-2} mpy was observed. Lowest corrosion rates were obtained in the control tests. This suggests that with increasing chloride, there is increase in the concentration of ions in the test solution which in turn leads to the degradation of MAS material in E20 with respect to the control test. The assertion is further established statistically through the analysis-of-variance (ANOVA) F-test. ANOVA, being an influential procedure for the analysis of experimental data, is suitable in factorial experimentations where numerous autonomous sources of variation might exist [22–24]. In this work, one-way ANOVA was used to assess the distinct and collective effects of the different concentrations of chloride (0, 32 and 64 mg/L) on the degradation degree of MAS in E20. Table 2 shows the results of the ANOVA test. It is seen that the experimentally determined mean-square ratio (35.0) is greater than the F ratio (30.8). Consequently, a conclusion can be made with 99% confidence, that there is significant variance between the mass losses of MAS samples tested in the three chloride concentrations based on the F-test result. That is to say, chloride concentration has significant effect on the mass loss of micro-alloyed steel in E20, within the tested range.

The increasing degradation of micro-alloyed steel due to chloride as detected in this study compares well with outcomes on corrosion performance of carbon steel in simulated fuel ethanol environment as reported in literature [11,21]. However, micro-alloyed steel may be supposed to be basically well-suited with E20 from the perspective of deterioration in fuel ethanol, since its corrosion rates are characteristically low and largely beneath the level of usual engineering significance intended for storing and handling applications [6]. Fig. 2 shows the morphology of MAS in as-received condition. The steel consists of mostly ferrite structure, alongside is lamellar pearlite arbitrarily distributed in the ferrite matrix. SEM image of MAS exposed to E20 + 0 mg/L NaCl revealed crazed cracks in MAS due to shrinkage of the sample surface as seen in Fig. 3. However, localized corrosion was noticeable on MAS at 32 and 64 mg/L NaCl concentrations (Figs. 4 and 5). Pitting (localized) corrosion was caused by the change in the ethanol environment due to the presence of aggressive chemical specie, particularly chloride ions. It must be pointed out that in the absence of chloride, no pitting was seen. This observation agrees with published results regarding the effect of chloride on mass loss of carbon steel in SFGE environment [11]. In addition, Figs. 3–5 show that E20 caused anodic dissolution of iron in the ferrite phase leaving a higher concentration of pearlite in mixed form.

Characterization of the corrosion products formed on MAS after exposure to E20

X-ray diffraction analysis of the corroded steels was carried out after mass loss tests in E20 with chloride. JCPDS software was used to recognize the existing chemical constituents in the oxide films. The corrosion products appeared as thick reddish layers covering the metal surface. Iron oxides deposited on a steel surface are usually a mixture of different oxides [21,25]. As such, characterization by XRD (Fig. 6) revealed the presence of lepidocrocite (γ-FeOOH), having a space group of Cmcm as reported in literature [11], hematite (Fe_2O_3) with an R-3c space group and iron (II) acetate in the corrosion products as shown in the XRD spectrum.

Table 2
ANOVA table showing the effect of chloride concentration on corrosion of MAS in E20.

Source of variation	Sum of squares	Degree of freedom	Mean square	Mean square ratio	Min. MSR at 99% confidence
Chloride concentration	0.21	2	0.105	35.0	30.8
Residual	0.01	3	0.003		
Total	0.21	5			

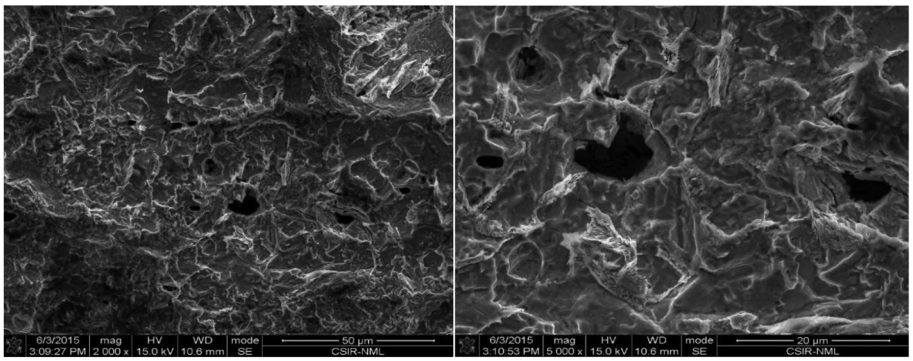

Fig. 4. Pitting on MAS after exposure to E20 with 32 mg/L NaCl.

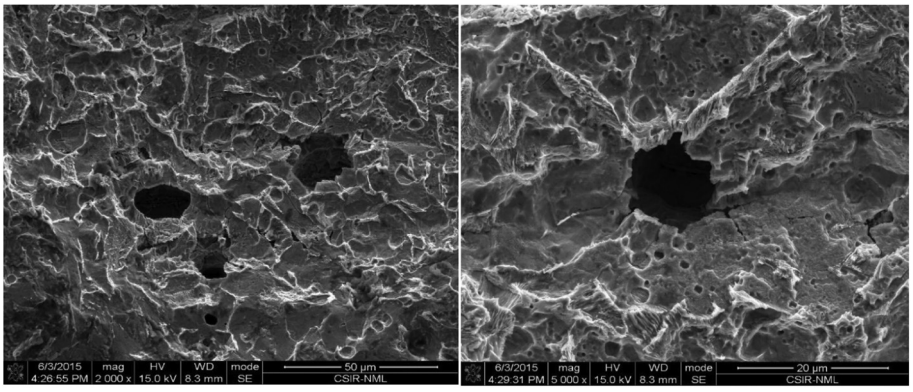

Fig. 5. Pitting on MAS after exposure to E20 with 64 mg/L NaCl.

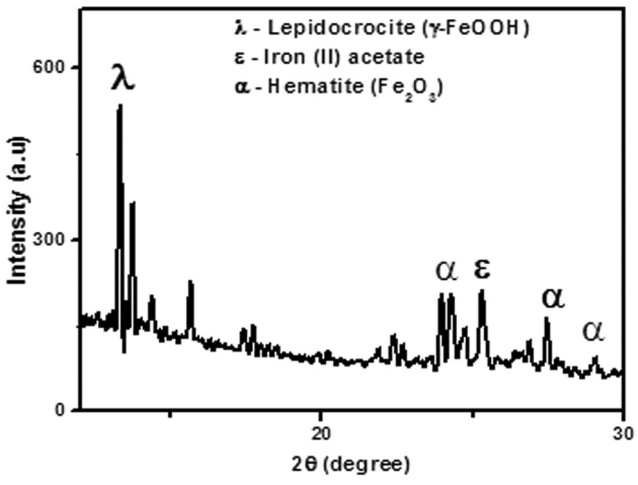

Fig. 6. Typical XRD analyses of corrosion products from MAS in E20 (with chloride) showing the presence of lepidocrocite, hematite and iron (II) acetate.

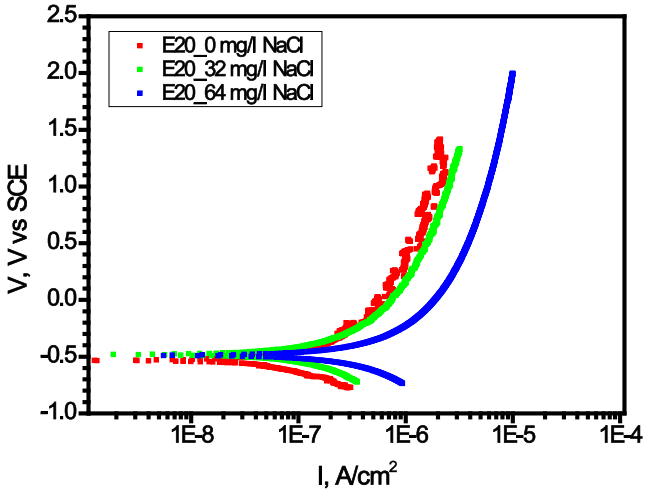

Fig. 7. Typical anodic polarization curves for MAS in E20 simulated fuel ethanol with variations in NaCl showing increased current density with chloride measured for MAS in E20.

Lepidocrocite being a semiconductor compound, is dynamic electrochemically besides considered not to possess protective properties [26]. Iron (II) acetate has also been reported to show high solubility in fuel grade ethanol environments [27] and consequently, has no protective function on the steel surface. The sites where iron (II) acetate exists are weak sites that encourage selective dissolution reaction and pitting corrosion. The formed films of the corrosion products were not adherent to the metal surface and so provided no protection to the substrate. In addition, the presence of iron in the corrosion products confirms that anodic dissolution of iron in ferrite took place during the mass loss tests.

Electrochemical tests

Potentiodynamic polarization was used to investigate the anodic polarization behavior of MAS. Reference electrochemical tests were carried out without chloride, then used as a base for investigating the effect of chloride on potentiodynamic polarization of

Table 3
Potentiodynamic polarization result showing the effect of chloride on MAS in E20 SFGE.

Test solution	E_{corr} (mV)	$I_{corr\text{-}estimate}$ (A/cm^2)	R_p (Ω)
E20 + 0 mg/L NaCl	−473	4.64×10^{-7}	791
E20 + 32 mg/L NaCl	−445	7.14×10^{-6}	443
E20 + 64 mg/L NaCl	−440	2.41×10^{-6}	163

MAS. The polarization curves obtained from the tests are shown in Fig. 7. MAS was not seen to exhibit a distinct passivation behavior and pitting potential with potentiodynamic polarization in the all the tests with the three chloride concentrations. This is expected since metals usually exhibit poor passive behavior in alcoholic environments [11]. In the absence of chloride, the polarization indicator (Fig. 7) shows fluctuations owing to very little ionic strength. Though, the signal becomes stronger as chloride increases. The polarization experiments were carried out at a scan rate of 2 mV/s to enable sufficient deterioration kinetics. From the analysis of the anodic and cathodic regions of the polarization curves, the E_{corr} and $I_{corr\text{-}estimates}$ were obtained at each chloride concentration as shown in Table 3.

In addition, the polarization resistance (R_p) which indicates the measure of the metal's resistance to corrosion under the various chloride conditions was determined from Eq. (2) [28].

$$R_p = \frac{\beta_a \beta_c}{2.3 I_{corr}(\beta_a + \beta_c)} \tag{2}$$

The evaluated current density ($I_{corr\text{-}estimate}$) measured from Tafel plots on the polarization curves, was seen to increase with increasing chloride concentration. This is in agreement with the corrosion rates obtained by immersion tests shown in Fig. 1. However, the results of Table 3 further indicate that the values of R_p which were obtained for the chloride based tests were lower than for the tests without chloride. Generally, the polarization resistance decreases with increasing concentration of chloride in solution due to decrease in resistance to charge-transfer reactions at the metal surface [29].

Conclusions

The aggressiveness of E20 simulated fuel ethanol blend on micro-alloyed steel has been considered, with variations in chloride concentration. The definite conclusions arrived at are as follows:

i. Chloride concentration of up to 64 mg/L increases the mass loss of MAS in E20. Chloride further increases the pitting tendency of MAS. In the absence of chloride, no pitting was observed.
ii. The current density of micro-alloyed steel increases as chloride ion increases in E20 simulated fuel ethanol environment.
iii. There is good correlation between electrochemical corrosion rates and mass loss corrosion rates of MAS in E20 simulated fuel ethanol environment.
iv. Micro-alloyed steel is supposed to be well-suited with E20 SFGE due to its very low corrosion rate.

Acknowledgments

This work was funded by the Council for Scientific and Industrial Research (CSIR), India and The World Academy of Sciences (TWAS), Italy (FR No. 3240275047). Covenant University is acknowledged for open-access funding.

References

[1] Lucio-Garcia MA, Gonzalez-Rodriguez JG, Casales M, Martinez L, Chacon-Nava JG, Neri-Flores MA, Martinez-Villafane A. Effect of heat treatment on H_2S corrosion of a micro-alloyed C-Mn steel. Corros Sci 2009;51:2380–6. http://dx.doi.org/10.1016/j.corsci.2009.06.022.
[2] Roman J, Vera R, Bagnara M, Carvajal AM, Aperador W. Effect of chloride ions on the corrosion of galvanized steel embedded in concrete prepared with cements of different composition. Int J Electrochem Sci 2014;9:580–92. Available online: www.electrochemsci.org/papers/vol9/90200580.pdf.
[3] Hansson CM, Frolund Th, Markussen JB. The effect of chloride cation type on the corrosion of steel in concrete by chloride salts. Cem Concr Res 1985;15:65–73. http://dx.doi.org/10.1016/0008-8846(85)90009-2.
[4] Pardo A, Otero E, Merino MC, Lopez MD, Utrilla MV, Moreno F. Influence of pH and chloride concentration on the pitting and crevice corrosion behavior of high-alloy stainless steels. Corros Eng 2000;56:411–8. http://dx.doi.org/10.5006/1.3280545.
[5] Park SA, Kim SH, Yoo YH, Kim JG. Effect of chloride ions on the corrosion behavior of low-alloy steel containing copper and antimony in sulfuric acid solution. Met Mater Int 2015;21:470–8. http://dx.doi.org/10.1007/s12540-015-4421-y.
[6] API Bulletin 939-E. Identification, repair, and mitigation of cracking of steel equipment in fuel ethanol service. 2nd ed. Washington, DC, USA: API; 2013.
[7] Sowards JW, Weeks TS, Mc Colskey JD. The influence of simulated fuel-grade ethanol on fatigue crack propagation in pipeline and storage-tank steels. Corros Sci 2013;75:415–25. http://dx.doi.org/10.1016/j.corsci.2013.06.026.
[8] Lou X, Yang D, Singh PM. Effect of ethanol chemistry on stress corrosion cracking of carbon steel in fuel-grade ethanol. Corrosion 2009;65:785–97. http://dx.doi.org/10.5006/1.3319105.
[9] Cao L, Frankel GS, Sridhar N. Effect of chloride on stress corrosion cracking susceptibility of carbon steel in simulated fuel grade ethanol. Electrochim Acta 2013;104:255–66. http://dx.doi.org/10.1016/j.electacta.2013.04.112.
[10] Cao L. Corrosion and stress corrosion cracking of carbon steel in simulated fuel grade ethanol [Ph.D. thesis]. United States: Ohio State University; 2012.
[11] Lou X, Singh PM. Role of water, acetic acid and chloride on corrosion and pitting behavior of carbon steel in fuel-grade ethanol. Corros Sci 2010;52:2303–15. http://dx.doi.org/10.1016/j.corsci.2010.03.034.
[12] Part V–VIII. In stress corrosion cracking of carbon steel in fuel-grade ethanol: review, experience survey, field monitoring and laboratory testing, 2nd ed. API Technical Report 939-D. Washington, DC, USA: API; 2013.
[13] Kane RD, Maldonado JG. Stress corrosion cracking in fuel ethanol: a recently recognized phenomenon. In: Proceedings of corrosion 2004, Paper No. 04543. Houston, Texas: NACE International; 2004.
[14] De Souza JP, Mattos OR, Sathler L, Takenouti H. Impedance measurements of corroding mild steel in an automotive fuel ethanol with and without inhibitor in a two and three electrode cell. Corros Sci 1987;27:1351–64. http://dx.doi.org/10.1016/0010-938X(87)90130-2.
[15] Prawoto Y, Ibrahim K, Wan Nik WB. Effect of pH and chloride concentration on the corrosion of duplex stainless steel. Arab J Sci Eng 2009;34:115–27. Available online: https://www.researchgate.net/publication/238739911 (accessed on 14 March 2016).
[16] Seikh EM, Seikh AH. Effects of grain refinement on the corrosion behavior of micro-alloyed steel in sulfuric acid solutions. Int J Electrochem Sci 2012;7:7567–78. Available online: www.electrochemsci.org/papers/vol7/7087567.pdf (accessed on 1 August 2012).
[17] ASTM D-4806-07. Standard specification for denatured fuel ethanol for blending with gasolines for use as automotive spark-ignition engine fuel. In: Annual book of ASTM standards. West Conshohocken, PA, USA: ASTM International; 2007.
[18] Joseph OO, Loto CA, Sivaprasad S, Ajayi JA, Tarafder S. Role of chloride in the corrosion and fracture behavior of micro-alloyed steel in E80 simulated fuel grade ethanol environment. Materials 2016;9:463. http://dx.doi.org/10.3390/ma9060463. Available online: http://www.mdpi.com/1996-1944/9/6/463 (accessed on 16 June 2016).
[19] Joseph OO, Loto CA, Sivaprasad S, Ajayi JA, Fayomi OSI. Comparative assessment of the degradation mechanism of micro-alloyed steel in E20 and E80 simulated fuel grade ethanol environments. In: AIP conference proceedings, vol. 1758. p. 020019-1–9-6. http://dx.doi.org/10.1063/1.4959395.
[20] ASTM G1-03. Standard practice for preparing, cleaning and evaluating corrosion test specimens. In: Annual book of ASTM standards. West Conshohocken, PA, USA: ASTM International; 2003.
[21] Baena LM, Gomez M, Calderon JA. Aggressiveness of a 20% bioethanol-80% gasoline mixture on autoparts: I behavior of metallic materials and evaluation of their electrochemical properties. Fuel 2012;95:320–8. http://dx.doi.org/10.1016/j.fuel.2011.12.002.
[22] Joseph OO, Alo FI. An assessment of the microstructure and mechanical properties of 0.26% low carbon steel under different cooling media: Analysis by one-way ANOVA. Ind Eng Lett 2014;4:39–45. Available online: http://www.iiste.org/Journals/index.php/IEL/article/view/14180 (accessed on 28 October 2016).
[23] Loto CA, Joseph OO, Loto RT, Popoola API. Corrosion inhibitive behavior of aluminium alloy in H_2SO_4. Int J Electrochem Sci 2014;9:1221–31. Available online: http://www.electrochemsci.org/papers/vol9/90301221.pdf.

[24] Loto CA, Joseph OO, Loto RT, Popoola API. Inhibition effect of Vernonia amygdalina extract on the corrosion of mild steel reinforcement in concrete in 0.2M H_2SO_4 environment. Eur J Environ Civ Eng 2013;17:1026–38. http://dx.doi.org/10.1080/19648189.2013.841596.

[25] Rincon A, De Rincon OT, Haces C, Furet NR, Corvo F. Evaluation of steel corrosion products in tropical climates. Corrosion 1997;53:28–35. Available online: https://www.onepetro.org/journal-paper/NACE-97110835.

[26] Jegdic B, Radovanovic SP, Ristic S, Alil A. Corrosion processes, nature and composition of corrosion products on iron artefacts of weaponry. Rev Sci Technol 2011;61:50–6. Available online: https://www.researchgate.net/publication/266227989 (accessed on 26 May 2015).

[27] Samusawa I, Shiotani K. Influence and role of ethanol minor constituents of fuel grade ethanol on corrosion behavior of carbon steels. Corros Sci 2015;90:266–75. http://dx.doi.org/10.1016/j.corsci.2014.10.020.

[28] Yahya S, Othman NK, Daud AR, Jalar A. Effect of scan rate on corrosion inhibition of carbon steel in the presence of rice straw extract. Sains Malaysiana 2014;43:1083–7. Available online: https://ukm.pure.elsevier.com/en/publications.

[29] Majed RA, Al-Kaisy HA, Al-Atrakchy HB. Effect of chloride ions on the corrosion behavior of Al-Zn alloy in NaOH solution at four different temperatures. Al-Khwarizmi Eng J 2008;4:26–36. Available online: https://www.researchgate.net/publication/268522470 (accessed on 25 November 2014).